Since January 2020 Elsevier has created a COVID-19 resource centre with free information in English and Mandarin on the novel coronavirus COVID-19. The COVID-19 resource centre is hosted on Elsevier Connect, the company's public news and information website.

Materials Science and Engineering C 48 (2015) 179–187

Contents lists available at ScienceDirect

Materials Science and Engineering C

journal homepage: www.elsevier.com/locate/msec

Silver nanoparticle-doped zirconia capillaries for enhanced bacterial filtration

Julia Wehling [a], Jan Köser [b], Patrick Lindner [c], Christian Lüder [c], Sascha Beutel [c], Stephen Kroll [a,*], Kurosch Rezwan [a]

[a] Advanced Ceramics, University of Bremen, Am Biologischen Garten 2, 28359 Bremen, Germany
[b] Department Sustainable Chemistry, Center for Environmental Research and Sustainable Technology, University of Bremen, Leobener Str. UFT, 28359 Bremen, Germany
[c] Institute for Technical Chemistry, Leibniz University of Hanover, Callinstr. 5, 30167 Hanover, Germany

ARTICLE INFO

Article history:
Received 11 August 2014
Received in revised form 17 October 2014
Accepted 1 December 2014
Available online 3 December 2014

Keywords:
Ceramic capillary membrane
Macroporous
Immobilized silver nanoparticles
Bactericide membrane surface
Silver leaching

ABSTRACT

Membrane clogging and biofilm formation are the most serious problems during water filtration. Silver nanoparticle (Ag_{nano}) coatings on filtration membranes can prevent bacterial adhesion and the initiation of biofilm formation. In this study, Ag_{nano} are immobilized via direct reduction on porous zirconia capillary membranes to generate a nanocomposite material combining the advantages of ceramics being chemically, thermally and mechanically stable with nanosilver, an efficient broadband bactericide for water decontamination. The filtration of bacterial suspensions of the fecal contaminant *Escherichia coli* reveals highly efficient bacterial retention capacities of the capillaries of 8 log reduction values, fulfilling the requirements on safe drinking water according to the U.S. Environmental Protection Agency. Maximum bacterial loading capacities of the capillary membranes are determined to be 3×10^9 bacterial cells/750 mm^2 capillary surface until back flushing is recommendable. The immobilized Ag_{nano} remain accessible and exhibit strong bactericidal properties by killing retained bacteria up to maximum bacterial loads of 6×10^8 bacterial cells/750 mm^2 capillary surface and the regenerated membranes regain filtration efficiencies of 95–100%. Silver release is moderate as only 0.8% of the initial silver loading is leached during a three-day filtration experiment leading to average silver contaminant levels of 100 μg/L.

1. Introduction

Water purification technologies play an important role in reducing the risk of the dissemination of waterborne diseases or epidemic outbreaks that are caused by pathogenic microorganisms and viruses. Bacteria such as pathogenic serovars of *Salmonella* and *Vibrio cholerae* are responsible for severe diseases such as typhoid fever and cholera, and *Escherichia coli* serves as an important indicator organism for fecal contaminations. Today, more than 250 serotypes of *E. coli* are known ranging from harmless gut commensals to severe pathogens [1], such as the virulent enterotoxigenic (ETEC), enteropathogenic (EPEC), and enterohemorrhagic (EHEC) *E. coli*. Furthermore, viral infections can be spread via drinking water contaminations and highly infectious diseases are for example hepatitis A, poliomyelitis caused by the poliovirus or the severe acute respiratory syndrome (SARS) which is caused by the coronavirus.

Because bacterial contaminations in drinking water are nowadays the main reason for most of the upcoming diseases [2], the removal and inactivation of pathogenic coliforms and other microorganisms are therefore a field of great interest for both, industries and local authorities. These institutions are obliged to fulfill the requirements on water containing 0 fecal and total coliform counts in 100 mL of water intended for drinking [3]. Hence, small-sized water filtration systems that can be easily transported and provide sufficient amounts of purified water are of global interest [4].

Different filtration materials have been described for the use in water purification, such as polymeric materials like cellulose acetate (CA) [5], polysulfone (PS) [6], polyacrylonitrile (PAN) [7] or polyvinylidene fluoride (PVDF) [8], while polyethersulfone (PES) is the most commonly used material for membrane applications [9]. In contrast to polymeric filter materials, ceramics feature outstanding positive properties because they are usually bio-inert, do not undergo swelling, are chemically and thermally stable, and withstand high mechanical stress enabling the cleaning and reuse of the filter after heat or acid/base treatment for decontamination [10,11]. These excellent properties result in an increased membrane service life compensating the higher costs of ceramics in comparison to polymeric materials.

The most common problem during bacteria filtration is the formation of biofilms on the membrane surface leading to pore clogging and consequently, a reduction of the filter performance is given. These clustered bacterial communities are attached to the membrane surface and protect themselves against environmental influences. Bacteria produce extracellular polymeric substances (EPS) to form complex macroscopic

* Corresponding author.
E-mail address: stephen.kroll@uni-bremen.de (S. Kroll).

http://dx.doi.org/10.1016/j.msec.2014.12.001
0928-4931/

structures that increase their resistance against e.g. toxic chemicals and antimicrobial agents. The removal of biofilms from the membrane surface is challenging and results in both cost- and time-intensive membrane regeneration procedures. Therefore, the reduction of the initial physical attraction of bacteria to the membrane surface, which can be attributed to a reversible attachment [1], plays a key role in inhibiting the formation of biofilms and several antibacterial surfaces have already been proposed [12,13]. Especially, immobilized nanosilver can act as an efficient antibacterial agent by killing retained bacteria directly on the membrane surface.

The decoration of filtration membranes with nanomaterials [14] have come into spotlight for water decontamination, catalysis and environmental remediation exploiting their unique surface chemical activities. Though the use of silver as an antimicrobial agent is known for about 7000 years [15], upcoming with the urgent need to eradicate antibiotic-resistant bacteria and with new insights into the mechanism of action [16], the use of silver has regained an emerged interest along with new interesting fields of applications [17]. Silver displays a broad antibacterial spectrum against Gram-positive and -negative bacteria [18] and nanosilver is one of the safest and mildest antibacterial agents for mammalian cells [19].

In recent years, silver nanoparticles (Ag_{nano}) have been embedded into various materials to generate antibacterial composites [20–23] and especially polymeric nanocomposite membranes are produced for water filtration purposes [6,14,24–27], since nanoparticles feature advantages in comparison to bulk silver: i) very small amounts of silver are needed due to the high specific surface area of silver nanoparticles, ii) when compared to silver ions, the bactericidal effect of Ag_{nano} is long-lasting because zerovalent (metallic) Ag_{nano} are not inactivated by complexation and precipitation [28] and iii) a controllable release of Ag^+-ions from the particles [29] compose them a cost-effective material for surface coatings. Most of the studies investigated the antibacterial properties of the nanocomposite membranes by describing the effect of the physical contact between silver nanoparticles and bacterial cells, but experiments were not performed under filtration conditions with special focus on antibacterial efficiency and silver leaching [27].

In our study, we present an advanced water filtration system based on ceramic capillary membranes which are subsequently doped with Ag_{nano}. Using zirconia as the membrane material and Ag_{nano} as the bactericidal coating, we combine a promising filtration material exhibiting high fracture toughness and bending strength with a highly effective antibacterial agent. Pore sizes of the capillary membrane of less than 0.2 μm and high open porosities of 51% enable the retention of bacterial cells during filtration [30]. Generated by direct reduction of silver nitrate on the membrane surface, immobilized Ag_{nano} display a bactericidal surface that kills filtrated bacteria directly on the membrane surface. Filtration experiments were performed by applying intracapillary feeding with bacterial suspensions and bacterial retention after different filtration times was determined using microbiological methods. The viability of retained bacteria was analyzed to evaluate the bactericidal action of immobilized Ag_{nano} and silver leaching during filtration was determined to consider eco-toxicological requirements.

2. Materials and methods

2.1. Preparation of Ag_{nano}-doped zirconia capillaries

Zirconia capillary membranes were fabricated by extrusion and sintered at 1050 °C for 2 h as described in our previous study [30]. As shown in Fig. 1, Ag_{nano} were immobilized on the membrane surface by a two-step immersion procedure according to the Creighton method [31] by direct reduction of silver ions on the surface of the capillaries. Capillaries featured an outer diameter (D_O) of 1.48 ± 0.01 mm, an inner diameter (D_I) of 0.90 ± 0.01 mm and an average wall thickness of 0.29 mm ± 0.01 mm. For all further tests, capillary pieces of 25 mm length were used which is in accordance with a weight of 82.9 ± 0.7 mg and a geometric surface area of 189 mm^2, except for the filtration experiment where 100 mm capillaries were applied (geometric surface area of 750 mm^2).

For the immobilization of Ag_{nano} one sintered capillary with a length of 25 mm was immersed in 2 mL silver nitrate ($AgNO_3$) solution (Sigma Aldrich, Germany, product number 209139) with varying concentrations from 2.5 to 10 mM at 25 °C and shaken at 1000 rpm for 5 min (pH was not adjusted). For the reduction of the immobilized silver ions, capillaries were subsequently immersed in 2 mL sodium borohydrate ($NaBH_4$) (Sigma Aldrich, Germany, product number 209139) for further 5 min. The reduction of the pre-immobilized silver ions was performed using a constant concentration of 2 mM $NaBH_4$. Prior to use, the $NaBH_4$ solution was stirred for 30 min at 25 °C followed by a cooling step to 4 °C without adjusting the pH. The number of immersion steps was varied between 1, 3, 5 and 10. Afterwards, the capillaries were washed twice in 15 mL of ddH_2O under shaking at 1000 rpm

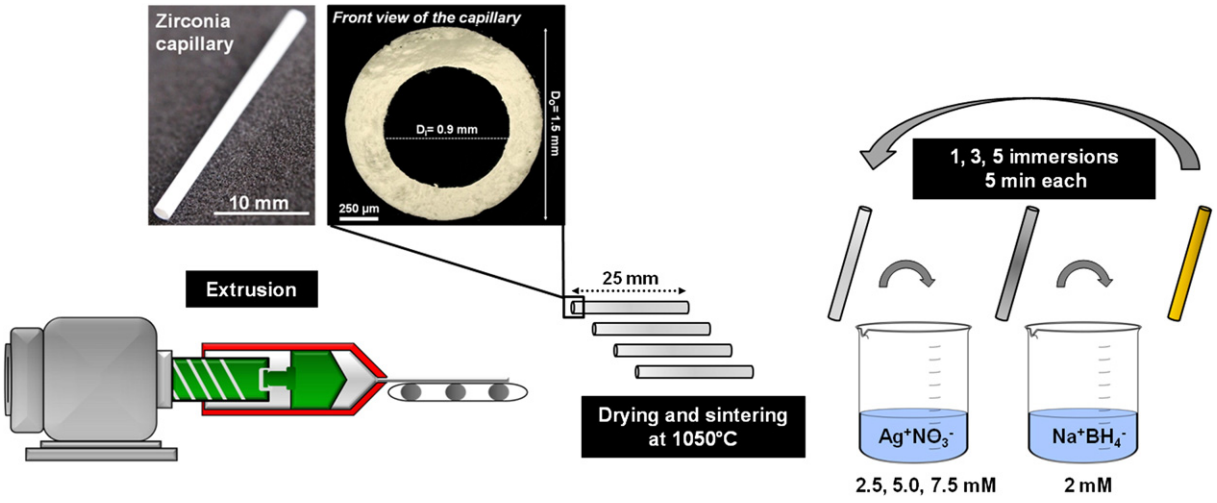

Fig. 1. Synthesis of zirconia capillaries by extrusion and immobilization of Ag_{nano} by reduction of $AgNO_3$ using $NaBH_4$. Zirconia capillaries with an outer diameter (D_O) of 1.48 ± 0.01 mm, an inner diameter (D_I) of 0.90 ± 0.01 mm and an average wall thickness of 0.29 mm ± 0.01 mm were fabricated by extrusion. The extruded capillaries were dried at room temperature for 2 days and the obtained green parts were sintered at 1050 °C for 2 h. Silver ions were directly reduced on the surface of the capillary membranes by immersion in $AgNO_3$ solution with varied concentrations and subsequently reduced in $NaBH_4$ at a constant concentration of 2 mM. This two-step immersion procedure was repeated 1–5 times to obtain adequate silver loading capacities.

for 5 min to remove unbound and weakly bound silver and finally dried at 70 °C for 30 min.

2.2. Silver loading capacities of Ag_{nano}-capillaries

Silver loading capacities were determined by three different methods: i) manual counting of immobilized Ag_{nano}, ii) image analysis using an image processing algorithm and iii) atomic absorption spectroscopy (AAS).

Scanning electron microscopy (SEM) micrographs of untreated and Ag_{nano}-capillaries were taken with a SEM Supra 40 (Carl Zeiss, Germany) operated at 2 kV. The chemical composition of both the membrane material and immobilized Ag_{nano} was recorded using an energy-dispersive X-ray spectroscopy (EDX) detector (BrukerXFlash 6| 30, Bruker Nano GmbH, Germany). The number of immobilized Ag_{nano} on the membrane surface was determined by manual counting using three different SEM micrographs for each membrane sample and four randomly chosen micrograph sections covering an area of 1 μm^2.

Additionally, the micrographs were analyzed using an image processing algorithm called "Silver-Particle Analyzer". The algorithm was developed in C# using Visual Studio 2012 with. NET 3.5 Framework and AForge.NET 1.7.0 Framework. The program used the characteristic gray-value distribution of the Ag_{nano} on the SEM micrographs. The analyses were carried out by screening the SEM images with a so-called top-hat filter. The top-hat filter is applied at a fixed size of 7×7 pixels which can be attributed to the size range of the Ag_{nano}. To consider exclusively the Ag_{nano} and no parts of the porous substrate, the contrast was increased and a threshold value for bright image segments was applied. The algorithm was used to quantify the percentage of Ag_{nano}-covered capillary surface and the total surface of bioactive silver based on the assumption that all Ag_{nano} were spherical. Results were compared with total silver loadings obtained from AAS analysis.

AAS measurements were performed to determine the total amount of immobilized Ag_{nano} on the surface of the capillaries. To quantify the silver loading, one 100 mm Ag_{nano}-capillary was acidified in 10% HNO_3 at 25 °C overnight. Due to applied acidic conditions, a complete release of the immobilized silver from the capillaries was enforced. An aliquot of 100 μL of the solution was stored at 4 °C until AAS measurements were performed (measurements were performed in triplicate using three individual capillaries). The silver loading was quantified by graphite furnace AAS using a Unicam 989 QZ AA Spectrometer with GF90 plus furnace and FS90 plus autosampler (Unicam, Cambridge, UK) after *aqua regia* digestion. The digestion was carried out by adding 80 μL of concentrated HCl (37%, p.a. VWR, Germany) and 20 μL of concentrated HNO_3 (≥65%, puriss p.a., Sigma-Aldrich, Germany) to the samples. After short mixing and centrifugation, the open samples were tempered at 56 °C overnight. The dry residue was dissolved in 1 mL diluted *aqua regia* (containing 10% HNO_3 and 19% HCl). Subsequently, the samples were measured after further dilution to be in the working range of the AAS (0.5–20 μg Ag L^{-1}).

2.3. Tests on antibacterial properties and filtration efficiencies of Ag_{nano}-capillaries

For all tests, bacterial suspensions of *E. coli* (Deutsche Sammlung von Mikroorganismen und Zellkulturen, Germany, DSMZ No. 1077) were prepared by inoculating a pre-culture in 70 mL of lysogeny broth (LB) (Sigma Aldrich Germany, No. L3022) for 16 h at 37 °C to allow a growth until the stationary phase is reached. Bacterial cells were washed once in OECD medium, which is used to simulate realistic surface water conditions [32] and the cell pellet collected by centrifugation was resuspended in OECD medium to obtain a realistic bacterial cell concentration of 10^8 cells/mL for wastewaters [33] according to McFarland standards [34]. Before use, capillaries were heat sterilized at 160 °C for 3 h. According to preliminary tests, this sterilization did not affect the bactericidal properties of the capillaries (data not shown).

2.3.1. Agar plate test

Ag_{nano} and untreated capillaries as a reference (each 25 mm length) were separately incubated in 4 mL *E. coli* suspensions at RT and 200 rpm for 30 min. After incubation, the capillaries were briefly washed in OECD medium to remove residual bacterial cells from the inner channel of the capillary (lumen), and subsequently placed on fresh LB plates containing 1.5% (w/w) agar. Incubation of the plates was performed at 37 °C for 24 h allowing the bacteria to grow.

2.3.2. Filtration test

Bacterial suspensions of *E. coli* were used for filtration purposes using untreated and Ag_{nano}-capillaries with accessible lengths of 100 mm, respectively. Filtration tests were performed in dead-end mode. Therefore, one end of the capillary was sealed with a two-component polydimethylsiloxane glue (Wirosil®, BEGO, Germany), while the other end of the capillary was connected to a convenient silicon tubing. Four individual capillaries (untreated vs. Ag_{nano}) and independent bacterial cultures were used. For intracapillary feeding with bacterial suspensions, a peristaltic pump (BVB Standard, Ismatec, Germany) was set to a constant flow rate of 250 μL min^{-1}. Permeates were collected and analyzed regarding the presence of bacterial cells using three different microbiological methods. Adenosin triphosphate was used as an indicator of bacterial metabolism and measured using a luciferase-based cell viability assay as described by Lara et al. [35]. 50 μL of the permeate was mixed with 50 μL of BacTiterGlo Assay (Promega No. G8231, Germany) and luminescence counts, directly correlating with the amount of present ATP, were recorded using a luminescence plate reader (Chameleon V, Hidex, Germany). Furthermore, the optical density of the bacterial suspension at 595 nm ($OD_{595\ nm}$) was measured using a plate reader (Chameleon V, Hidex, Germany). Colony forming units (CFU) were determined by plating the undiluted permeate onto agar plates (Coliform Count Plate, Petrifilm, 3 M, Germany) and CFUs were counted after an incubation at 37 °C for 24 h. All experiments involving ATP assay, OD measurements, and CFU tests were performed using three replicates. Obtained results based on permeate samples were compared with those from the bacterial feed solution which were set as 100% survival of bacteria cells.

Preliminary results showed that capillaries stood a bacterial load which was corresponding to a membrane flux reduction of 30%, which was reached after 150 min. Consequently, filtration was stopped after 150 min and back flushing was initiated to remove retained bacterial cells from the inner capillary membrane surface. For this, capillaries were immersed into fresh OECD medium and the peristaltic pump was operated in back flush mode with a membrane flux of 1.27 mL min^{-1} for 1/10 of the filtration time, in this case i.e. 15 min. The back flushed suspension was analyzed by using ATP assay, OD measurement and determination of CFU as described before to determine the bacterial viability of the recovered bacterial cells. The back flushed volume was determined and correlated with the filtration volume of each individual capillary for further calculations.

2.3.3. Silver leaching during filtration

Silver leaching from Ag_{nano}-capillary membranes during filtration was analyzed by determining the silver content of bacteria-free permeate samples via AAS after filtration times of 30 min, 1 h and 2 h, respectively. The filtration conditions (i.e. bacterial feed concentration, buffer, applied flow rate) as well as the length of Ag_{nano}-capillaries were the same compared to the bacterial filtration tests described in Section 2.3.2. For statistical significance three individual capillary membranes were analyzed and permeate samples were collected on three consecutive days where one filtration cycle was performed per day. After each filtration cycle, back flushing was applied for membrane regeneration. For this, capillaries were immersed into fresh OECD medium and the peristaltic pump was operated in back flush mode with a flow rate of 1.27 mL/min for 1/10 of the filtration time (i.e. 12 min). During the time between back flushing and a new filtration cycle the capillaries

were held humid and stored at 4 °C over night to provide stable conditions. For AAS measurements 100 μL of the permeate samples was immediately acidified after filtration by adding 10 μL HNO_3 (1%) and stored at 4 °C. Afterwards, AAS measurements were performed as described in Section 2.2 and untreated capillary membranes served as controls for all experiments.

3. Results and discussion

3.1. Surface properties of Ag_{nano}-ceramic capillary membranes

Zirconia capillary membranes were fabricated by extrusion as described in our previous work [30] and functionalized with Ag_{nano} in a straightforward two-step procedure via direct reduction of $AgNO_3$ on the capillary surface. As shown in Fig. 2A, the presence of Ag_{nano} on the capillary changed the color of the surface from white (non-functionalized capillary made of zirconia) to yellow indicating a homogeneous surface coating. SEM micrographs demonstrate the presence of homogenously distributed Ag_{nano} on the capillary outer surface (Fig. 2C), whereas the microstructure of the surface of a non-functionalized capillary is shown in Fig. 2B. EDX analysis confirmed that the immobilized nanoparticles on the membrane surface consisted of silver (Fig. 2C, inset). In addition, SEM micrographs of the inner surface of capillaries produced by using 5 mM $AgNO_3$ and 5 immersion cycles were taken and displayed a similar Ag_{nano} loading (Supplementary Information, Fig. S1).

3.2. Loading capacities of immobilized Ag_{nano} on ceramic capillary membranes

Yielding a high Ag_{nano} loading on the membrane surface, different $AgNO_3$ concentrations in the range between 2.5 and 10 mM and different numbers of immersion cycles (1, 3, 5 and 10 immersions, respectively) were applied, whereas the incubation time (5 min) and the concentration of the reduction solution $NaBH_4$ (2 mM) were held constant. For quantification of immobilized Ag_{nano} on the membrane surface, three different methods were employed: manual counting of Ag_{nano} on randomly chosen sections of SEM micrographs, image analysis of SEM micrographs using the software tool "Silver-Particle Analyzer" and atomic absorption spectroscopy (AAS).

As shown in Fig. 3A, manual counting revealed that the highest loading capacity of 1702 ± 91 Ag_{nano} per μm^2 capillary was achieved when using a 5 mM $AgNO_3$ solution in combination with five successional immersion steps, alternating membrane incubation in $AgNO_3$ solution and in the reduction solution $NaBH_4$. In general, regarding one particular $AgNO_3$ concentration (2.5 mM, 5 mM and 7.5 mM, respectively),

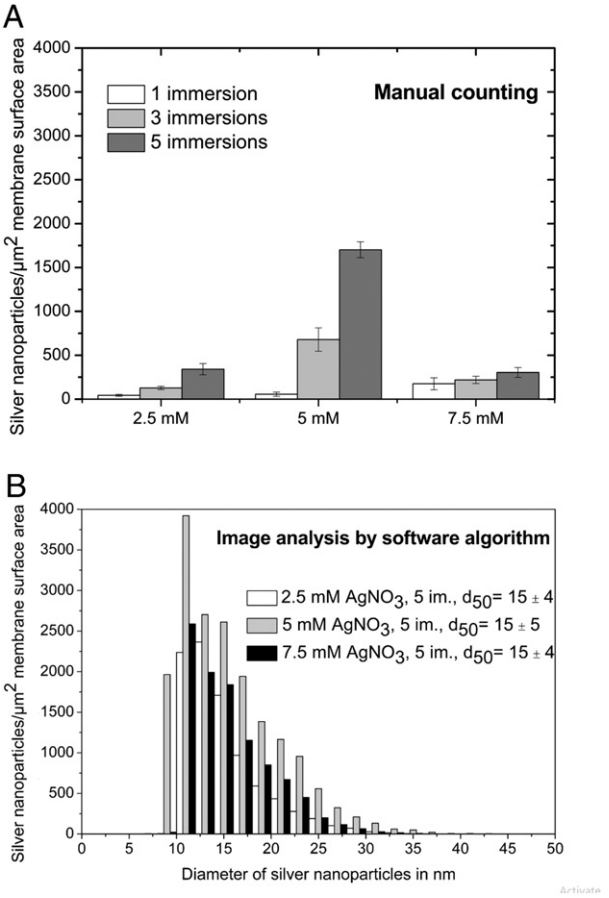

Fig. 3. Quantification of immobilized Ag_{nano} on the capillary surface. Assessment of the number of Ag_{nano} on the surface of the capillary membranes derived from manual counting of four different regions on three different SEM micrographs covering an area of 1 μm^2 each (A). Ag_{nano} size distribution covering an area of 1 μm^2 capillary obtained by image analysis software (B).

increased numbers of immersion steps led to increased numbers of immobilized Ag_{nano}. Compared to an initial $AgNO_3$ concentration of 2.5 mM, Ag_{nano}-doped membranes fabricated by using 5 mM $AgNO_3$ showed higher loading capacities by a factor of 1.3 (one immersion), 5.3 (three immersions) and 5.0 (five immersions), respectively. An increase of the $AgNO_3$ concentration to 7.5 mM did not further increase the Ag_{nano} loading on the membrane and loading capacities were in the same order of magnitude compared to 2.5 mM $AgNO_3$. The

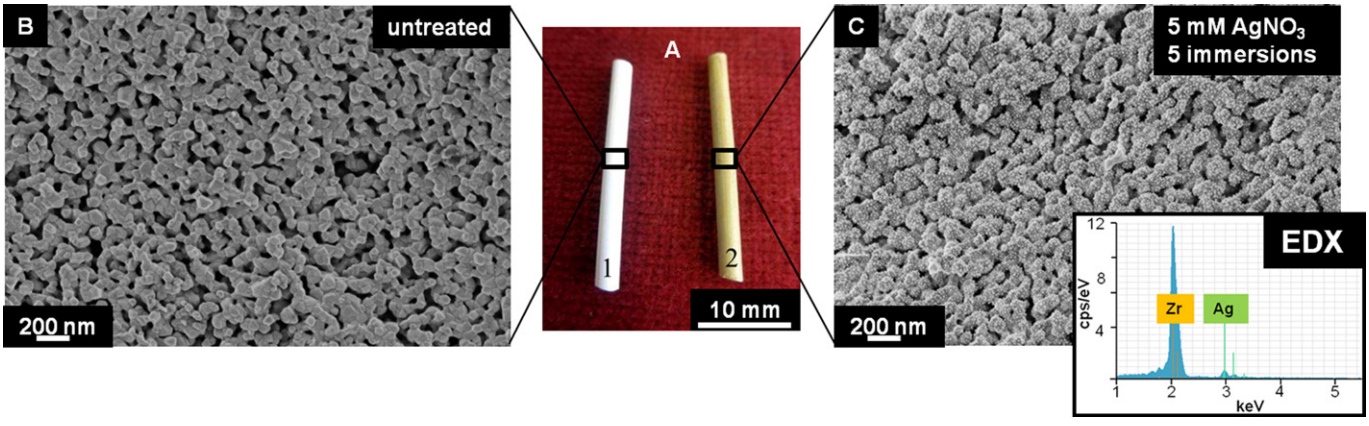

Fig. 2. Untreated and Ag_{nano}-ceramic capillary membranes. Direct formation of Ag_{nano} on the surface of zirconia capillaries leads to a color change from white, displaying the non-functionalized capillary, to yellow (A). Ag_{nano} were generated by 5 immersion cycles using 5 mM $AgNO_3$ and 2 mM $NaBH_4$. SEM micrographs confirm the presence of homogeneously distributed Ag_{nano} on the functionalized capillary (C), whereas the microstructure of a non-functionalized capillary is shown in part B. EDX analysis revealed the presence of silver on the functionalized membrane surface (C, inset).

application of a higher concentration of 10 mM $AgNO_3$ and 10 immersion cycles led to the undesired formation of agglomerates of immobilized Ag_{nano}, which were inhomogeneously distributed on the capillary surface (data not shown). Providing high Ag_{nano} loadings in combination with a homogeneous membrane surface coating the application of five immersion cycles is the method of choice.

Additionally, image analysis software was applied to quantify the particle size distribution of immobilized Ag_{nano} on the membrane surface (Fig. 3B). Results stood in good correspondence with the results derived from manual counting (Fig. 3A) exhibiting the highest number of Ag_{nano} on capillaries generated by using 5 immersion steps in 5 mM $AgNO_3$ (Fig. 3B, Supplemental information, Table S1). Silver particle sizes were in the range of approximately 9–35 nm and the average particle diameter for the applied production conditions was calculated to be $d_{50} = 15$ nm (Fig. 3B) indicating that different $AgNO_3$ concentrations from 2.5 to 7.5 mM lead to similar silver particle sizes and morphologies.

Referring to a geometric surface area of 1 mm^2 on Ag_{nano}-capillaries, the active silver surface on the outer and inner surface of the capillary was calculated to allow an assessment of the total silver surface that can interact with the filtrated bacterial cells. For the calculation based on the particle area that was recognized by the analysis software, it was assumed that all Ag_{nano} were spherical and the contact area between the nanoparticles and the capillary surface was negligible. Again, the highest accessible silver surface area of 0.594 mm^2 was present on capillaries treated with 5 mM $AgNO_3$, whereas capillaries treated with 2.5 mM and 7.5 mM exhibited a total silver surface of 0.269 and 0.314 mm^2, respectively. Implicating the density of silver (10.49 g/cm^3), total amounts of silver were calculated and capillaries treated with 5 mM $AgNO_3$ and 5 immersion steps yielded the highest silver loadings of 20 ng per 1 mm^2 geometric surface area (Table 1).

The two methods, manual counting and software generated particle counts, only consider the Ag_{nano} distribution on the geometric outer and inner surface of the ceramic capillary based on SEM micrographs. The possible penetration of Ag_{nano} into the pores of the membrane material was therefore not considered. With regard to this, we additionally determined the total silver loadings of capillaries treated with 5 mM $AgNO_3$ by AAS. Using this method, an acidic digestion ensured the total release of silver from the capillaries. With regard to the surface of the pores, the measured amounts of total silver loadings were correlated to the specific surface area of Ag_{nano}-capillaries of 7.05 m^2/g (Supplemental information, Table S2). The obtained AAS results were comparable to the results derived from counting: total Ag_{nano} loadings increased with the number of immersions featuring 0.048 ± 0.001 ng silver/mm^2 specific surface area for 1 immersion, 0.123 ± 0.004 ng silver/mm^2 of capillary specific surface area for 3 immersions and 0.176 ± 0.040 ng silver/mm^2 of capillary specific surface area for 5 immersions (Fig. 4A). It is noticeable that the calculated amount of bioactive silver based on pixel-generated data of 20 ng per 1 mm^2 geometric surface area was significantly higher than the total amount of silver of 0.18 ng per 1 mm^2 specific surface area that was measured via AAS. The discrepancy of the results can be explained by the different reference membrane areas that were applied. Results from the counting method must be referred to the geometric surface area, since only Ag_{nano} on the outer membrane of the capillaries were considered for the counting. Fig. 4B and C clearly display that Ag_{nano} penetrated to a large extent into the pores of the capillary membrane. For that reason, for the determination of total silver loadings via AAS, the specific surface area determined via nitrogen-adsorption was considered as a reference leading to significantly lower values. Simultaneously, the deep penetration of Ag_{nano} into the pores displays an advantage by enhancing the accessible interaction surface of bactericidal Ag_{nano} and filtrated bacteria.

Membrane pore size distributions as well as pore volumes and mechanical properties of untreated and Ag_{nano}-capillaries (5 mM $AgNO_3$, 5 immersion steps) were determined by nitrogen adsorption isotherms (BET–BJH evaluation) and bending strength tests (3-point bending test). Results showed that the additional Ag_{nano}-functionalization did not significantly alter both, the membrane pore sizes and the mechanical properties of the zirconia capillaries [30] providing an efficient filtration performance and good mechanical properties for handling purposes (Supplemental information, Table S2, Fig. S2).

Table 1
Accessible silver surface area and total amount of immobilized silver on 1 mm^2 geometric surface area of Ag_{nano}-capillaries.

Conditions for the immobilization of silver nanoparticles	Accessible silver surface area in mm^2[a]	Total amount of silver in ng[b]
2.5 mM $AgNO_3$, 5 immersions	0.269 ± 0.076	8.23 ± 2.51
5 mM $AgNO_3$, 5 immersions	0.594 ± 0.129	20.00 ± 5.08
7.5 mM $AgNO_3$, 5 immersions	0.314 ± 0.101	9.95 ± 3.90

[a] The accessible silver surface area was calculated based on software-calculated pixel areas and on the assumption that all Ag_{nano} were spherical.
[b] The total amount of immobilized Ag_{nano} was calculated considering the density of silver (10.49 g/cm^3).

3.3. Bactericidal properties of Ag_{nano}-capillaries under batch and filtration conditions

Bactericidal properties of Ag_{nano}-capillaries were analyzed by incubating untreated and Ag_{nano}-capillaries in bacterial suspensions of *E. coli* for 30 min at room temperature. As expected, bacterial growth was only visible close to the untreated capillaries, whereas Ag_{nano}-capillaries prevented the growth of *E. coli* cells displaying significant bactericidal properties (Fig. 5).

For realistic fresh water filtration conditions the standardized OECD medium was chosen for the preparation of the bacterial feed, since it is used for experiments with the freshwater algae *Pseudokirchneriella subcapitata* [36]. Filtration of an *E. coli* suspension was performed in dead-end mode by intracapillary feeding at an initial flow rate of 250 μL/min for 2.5 h using 100 mm capillaries (exhibiting a geometric surface area of 750 mm^2) and the resulting permeates of untreated and Ag_{nano}-capillaries were analyzed every 30 min regarding bacterial viability by measuring ATP levels, CFU and $OD_{595\ nm}$. Results showed highly efficient filtration efficiencies for untreated and Ag_{nano}-capillaries achieving a bacterial retention of nearly 100% which corresponds to a $\log_{10}$ reduction value (LRV) of 8 (Fig. 6A, B). No CFUs were detected after plating the permeate samples onto agar plates and ATP and $OD_{595\ nm}$ levels of the permeate samples were comparable to the buffer controls indicating a clear and bacteria-free solution (data not shown). Achieving $\log_{10}$ reduction levels of >6, the here presented capillaries accomplish the bacteria filter criterion for safe and clean drinking water according to the U.S. Environmental Protection Agency [37].

Since the membrane flux decreased during filtration, back flushing was induced for membrane regeneration after the filtration of approximately 3×10^9 bacterial cells per capillary (750 mm^2 geometric surface area), which corresponds to a filtration time of 2.5 h. Back flushing was applied for 1/10 of the filtration time and filtration efficiencies were recovered by reaching 95–100% of the initial membrane flux (Fig. 6A, B).

Since both, untreated and Ag_{nano}-capillaries, featured similar filtration properties, the assumed benefit of the Ag_{nano}-immobilization is the inhibition of the initial attachment of living bacteria [38,39] to the capillary surface and the inhibition of initial biofilm formation. In general, after initial attachment, bacteria start to secrete extracellular polymeric substances providing a matrix for other bacteria to embed and build a biofilm [40]. This biofilm leads to pore blocking which is followed by an increase of the transmembrane pressure and operating time leading to lower filtration efficiencies. Creating a strong bactericidal surface by using an Ag_{nano} coating, bacteria are assumed to die when coming into contact with the capillary membrane before the expression of biofilm components will be initiated and dead bacteria will be removed by operating the pump in back flush mode [41].

To analyze the viability of the retained bacteria, the recovered bacteria from back flushing were analyzed regarding ATP levels and CFU.

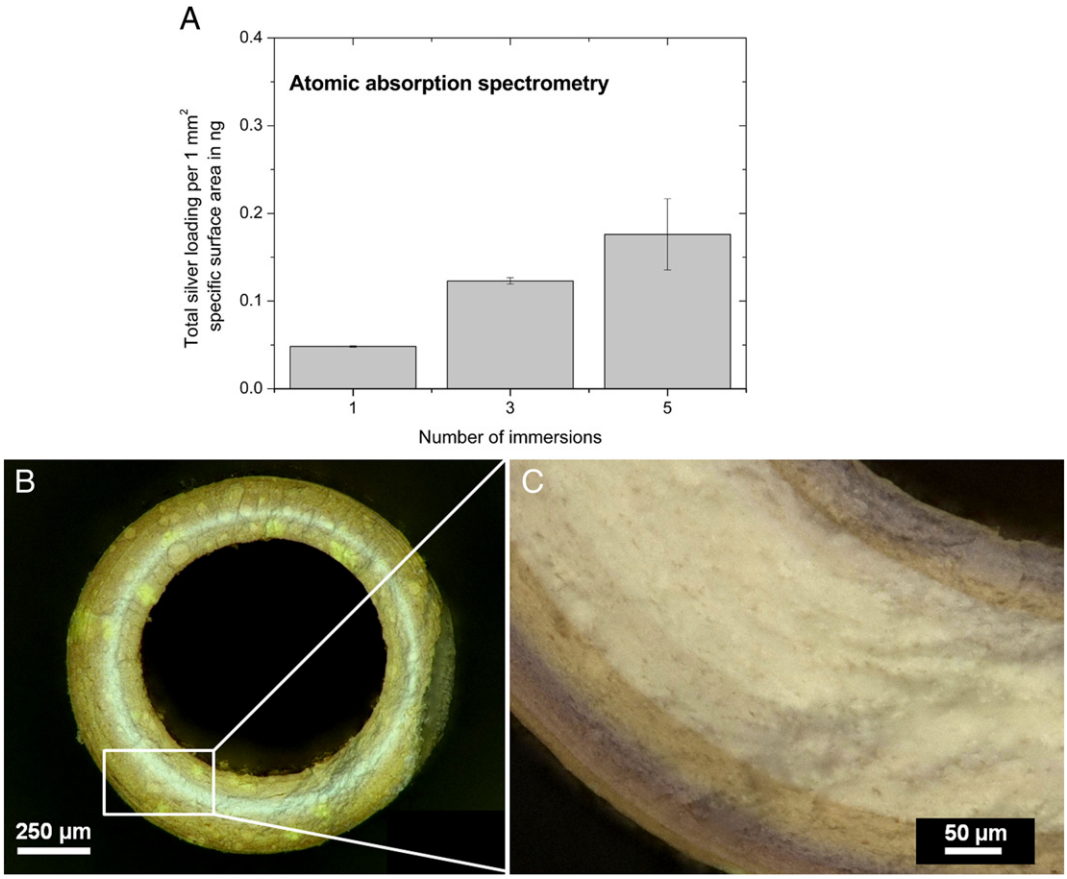

Fig. 4. Total amount of immobilized Ag_{nano} per 1 mm^2 specific surface area measured via AAS and penetration of immobilized Ag_{nano} into the membrane material (5 mM $AgNO_3$, 5 immersions). AAS revealed total silver loadings of capillary membranes that were produced using 5 mM $AgNO_3$ and varying numbers of applied immersions (A). Cross section of a Ag_{nano}-doped capillary membrane where the intensity of the yellow coloration is correlated with the content of immobilized silver nanoparticles (B, C).

Unfortunately, bacteria that were recovered from Ag_{nano}-capillaries during back flushing after 150 min filtration were found to be viable as measured by ATP levels and CFU. The amount of filtrated bacteria was probably too high so that the contact of bacterial cells with the bactericidal Ag_{nano} surface could not be assured (data not shown).

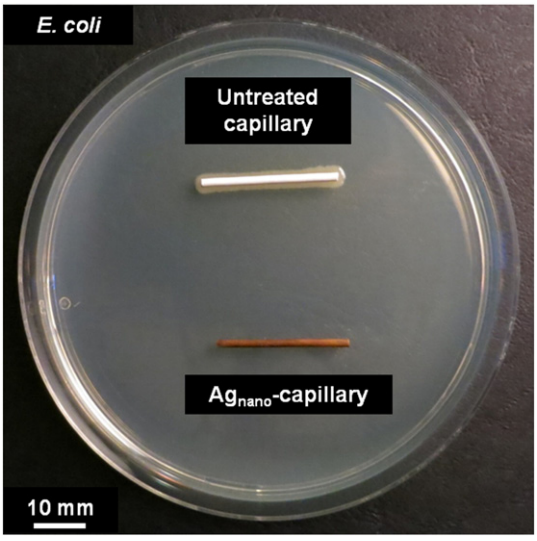

Fig. 5. Bactericidal properties of Ag_{nano}-capillary membranes. An agar plate test displays the bactericidal properties of the Ag_{nano}-capillaries (5 mM $AgNO_3$, 5 immersion cycles) against Gram-negative *E. coli*. While considerable bacterial growth was observed close to the untreated capillaries, the Ag_{nano}-capillaries exhibited no bacterial growth.

Therefore, individual Ag_{nano}-capillaries were tested for filtration times of 30, 60, 90, 120 and 150 min to identify the maximum filtration time that ensured the death of retained bacteria. Back flushing after 30 min and 60 min filtration time showed that recovered *E. coli* cells from Ag_{nano}-capillaries were dead displaying marginal bacterial ATP levels of 3.4 and 1.6% in comparison to reference bacteria that were recovered from untreated capillaries (Fig. 6C). Capillaries that were used for longer filtration times of >60 min were not capable in killing bacterial cells at the inner membrane surface of the capillaries as shown by determined ATP levels (Fig. 6C). Back flushing of Ag_{nano}-capillaries should therefore be initiated after a maximum filtration time of 60 min, corresponding to a bacterial load of 6×10^8 bacterial cells/750 mm^2 geometric capillary surface area.

Understanding the stability of each individual bactericidal Ag_{nano} membrane coating, Ag_{nano}-capillary membranes were tested for five consecutive filtration cycles of 60 min each, while back flushing was initiated after each cycle. Microbiological results showed that bacterial viability was decreased to 2–5% in relation to the reference bacteria that were recovered from untreated capillary membranes as analyzed by ATP levels and CFU indicating a stable bactericidal membrane surface at suitable filtration times of 60 min (Fig. 6D).

Similar results were obtained by Liu et al. [20] showing that a silver-nanoparticle-decorated polysulfone membranes exhibited anti-adhesive properties in comparison to unfunctionalized polysulfone membranes. Although the authors reported similar retention rates for unfunctionalized and silver-functionalized polysulfone membranes, significantly more bacteria were detached during rinsing experiments from the silver-decorated membranes than from untreated membranes. However, our back flushing results (Fig. 6C) also showed that longer filtration times >60 min were not recommendable, since bacterial killing

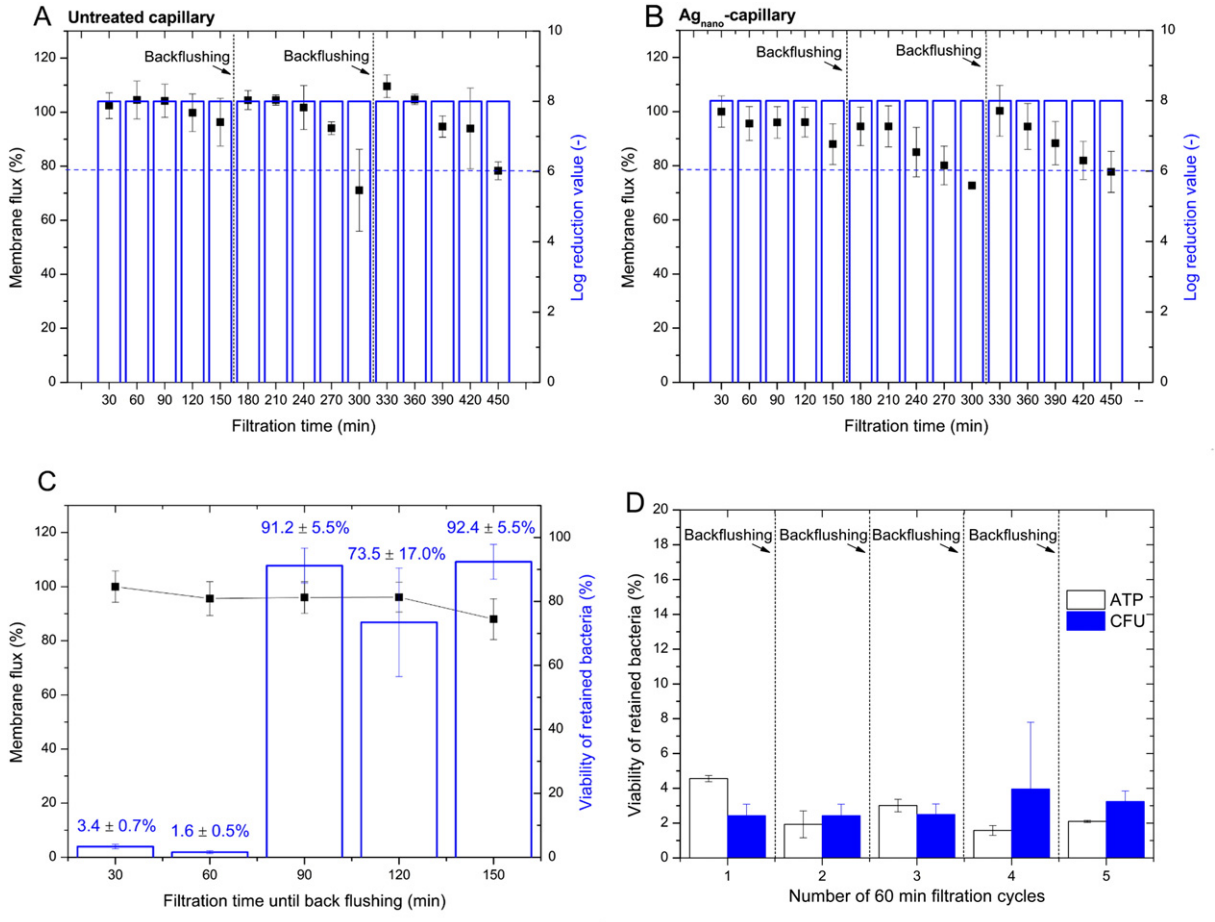

Fig. 6. Filtration efficiencies of untreated and Ag_{nano}-capillaries. Filtration in dead-end mode by intracapillary bacterial feeding was performed using untreated (A) and Ag_{nano}-capillary membranes (B) resulting in bacterial retention values of $\log_{10}$ 8. The blue, dashed line indicates the requirements on safe and clean drinking water of log reduction values of 6 according to the U.S. Environmental Protection Agency. Back flushing was applied after a filtration time of 2.5 h, corresponding to approximately 3×10^9 cells, resulting in regained membrane fluxes of 95–100%. No significant differences in bacterial retention rates ensuring log reduction values of 8 were obtained for untreated versus Ag_{nano}-capillary membranes (A, B). Individual Ag_{nano}-capillaries were used for different filtration times to identify the maximum filtration time that still guaranteed the killing of retained bacteria: filtration times of ≤60 min allowed the killing of filtrated bacteria (C). Regarding the stability of the bactericidal membrane coating, Ag_{nano}-capillaries were efficient in killing retained bacteria after five consecutive filtration cycles of 60 min each, where back flushing was applied for membrane regeneration (D).

was not ensured anymore. The bacterial filter cake was probably too thick to allow a contact-induced killing of bacteria by Ag_{nano}.

Silver contamination of water is an environmental predicament. Since silver is proved to be toxic against several freshwater organisms such as *Daphnia magna* [42] and may lead to safety concerns [43], its release into the environment needs to be accurately monitored.

Thus, the release of silver from the Ag_{nano}-capillaries during filtration and silver maximum contaminant levels were determined. Therefore, samples from the filtrated permeates of three individual capillaries were removed after 30 min, 60 min and 120 min of filtration on three consecutive days and analyzed by AAS. AAS measurements revealed that the silver release was highest at the beginning of the filtration on each individual day. After the first burst release after 30 min of filtration on the first day where 400 ± 3 μg/L of silver was released, silver leaching progressively decreased reaching values of 34 ± 0 μg/L already after 60 min of filtration and only 21 ± 17 μg/L at the last measurement after 420 min of filtration (Fig. 7). Among the filtration cycles, capillaries were stored under humid conditions at 4 °C overnight until filtration was started again. The storage induced a continuous release of silver from the capillary, which was then released at the following filtration cycles, which explains the recurring increases of silver release in the beginning of each filtration cycle. High standard deviations result from the phenomenon that small pieces of the capillaries got lost and were measured in the permeate samples. The maximum contaminant level for silver in drinking water is 50 μg/L as set by the World Health Organization (WHO), whereas "under special situations where silver salts are used to maintain the bacteriological quality of drinking-water higher levels of up to 100 μg/L can be tolerated without risk to health" [44]. Although silver was continuously released during filtration, WHO requirements were fulfilled already after 1 h of filtration when silver contaminant levels of 34 ± 0 μg/L were reached.

In addition to the eco-toxicological aspect, the loss of the bactericidal coating displays a drawback, because it reduces the operating time and requires a frequent replacement of the coating or the complete membrane. Total silver loading capacities of Ag_{nano}-capillaries of 411.64 ± 94.88 μg silver/100 mm capillary were determined by AAS. The filtration experiment showed that 0.23 ± 0.05% of the initial silver loading was released after the first 30 min of filtration and amounts of 0.01 ± 0.05% were released after 420 min of filtration on the third day. The total silver release during the three-day experiment was determined to be 0.81 ± 0.43% of the initial silver content that was immobilized on each capillary displaying a very good stability of the bactericidal Ag_{nano} coating.

Leaching of immobilized silver has also been demonstrated by Chou et al. [45] who analyzed the stability of an Ag_{nano} coating on cellulose acetate hollow fiber membranes. A 180 day static immersion in water decreased the silver content on the membrane surface by 90%, but still an antibacterial effect against *E. coli* and *Staphylococcus aureus* was evident.

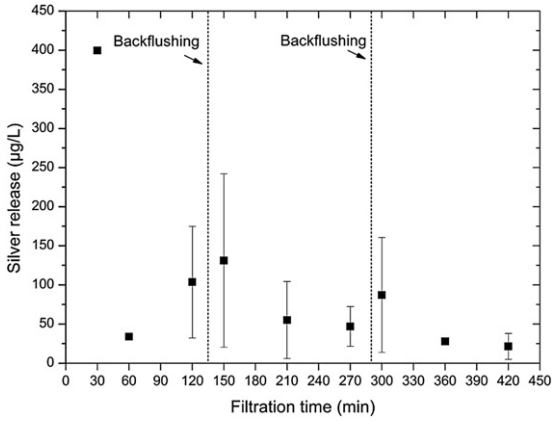

Fig. 7. Silver release during filtration. Silver contents in the permeate samples of three individual capillaries of 100 mm lengths were analyzed using AAS to determine the silver release from the Ag_{nano}-capillaries. For this, permeate samples were removed after 30 min, 60 min and 120 min of filtration on three consecutive days. Silver leaching was highest at the beginning of the three filtration cycles and decreased progressively during each filtration cycle.

In contrast, after permeating with water for 5 days, a significant higher and faster loss of silver was determined and no antibacterial effect was measurable anymore. Other studies also reported rapid depletions of silver from membrane surfaces after relatively short filtration periods (0.4 L/cm^2) and the soon loss of antibacterial and antiviral activities [6]. The here presented capillaries were capable of killing bacteria during filtration for at least five consecutive filtration cycles of 60 min and the silver release from the membrane after the first 30 min of filtration fulfilled the requirements on eco-toxicological demands.

4. Conclusions

Porous ceramic capillaries made of zirconia were functionalized with broadband bactericidal Ag_{nano} for utilization as small-sized water purification modules exhibiting durable antibacterial properties. The immobilization of Ag_{nano} was performed via direct reduction of silver nitrate to metallic Ag_{nano} on the surface of the capillaries. This straightforward procedure led to high silver loadings of up to 1700 Ag_{nano} per µm^2 capillary surface when using 5 mM $AgNO_3$ and 5 immersion cycles and could also be transferred to other oxide and non-oxide ceramics, such as aluminum oxide or silicon carbide. Total silver loadings as determined by AAS were found to be 0.18 ng silver per 1 mm^2 specific surface area and 20 ng silver per 1 mm^2 geometric surface area as calculated based on nanoparticle-covered membrane surface areas.

Zirconia capillaries exhibited excellent filtration performances obtaining bacterial retention rates of $\log_{10}$ reduction values of 8. Back flushing cycles of 1/10 of the filtration time were suggested for membrane regeneration leading to regained filtration efficiencies of 95–100%.

Creating a strong bactericidal surface, immobilized Ag_{nano} on the zirconia surface efficiently killed bacteria during filtration for filtration times of up to 60 min corresponding to 6×10^8 filtrated bacterial cells/750 mm^2 capillary surface. A subsequent back flushing cycle ensured the removal of dead cells from the membrane surface leading to the regeneration of filtration efficiencies and allowed the application for consecutive filtration cycles. Release of silver during filtration was analyzed and was moderate leading to silver contaminant levels of 34 µg/L after 1 h of filtration (250 µL/min).

Displaying strong bactericidal properties, the described ceramic–silver composite might be beneficial for several disinfection strategies, for example when applied for the coating of medical devices or for areas in which germ-free surfaces are necessary.

Acknowledgments

Financial support from the Federal Ministry of Education and Research (BMBF, support code 0315520) is gratefully acknowledged. We thank Petra Witte (University of Bremen, Department of Geosciences) for her support with the SEM.

Appendix A. Supplementary data

Supplementary data to this article can be found online at http://dx.doi.org/10.1016/j.msec.2014.12.001.

References

[1] C. Beloin, A. Roux, J.M. Ghigo, *Escherichia coli* biofilms, Curr. Top. Microbiol. 322 (2008) 249–289.
[2] E. Butler, A. Silva, K. Horton, Z. Rom, M. Chwatko, A. Havasov, J.R. McCutcheon, Point of use water treatment with forward osmosis for emergency relief, Desalination 312 (2013) 23–30.
[3] P. Jain, T. Pradeep, Potential of silver nanoparticle-coated polyurethane foam as an antibacterial water filter, Biotechnol. Bioeng. 90 (2005) 59–63.
[4] J.E. Rademan, Patent: Combinations of liquid filtration media and methods for enhanced filtration of selected water contaminants, RH Black-US Patent 20,130,022,686, (2013).
[5] C.X. Liu, D.R. Zhang, Y. He, X.S. Zhao, R. Bai, Modification of membrane surface for anti-biofouling performance: effect of anti-adhesion and anti-bacteria approaches, J. Membr. Sci. 346 (2010) 121–130.
[6] K. Zodrow, L. Brunet, S. Mahendra, D. Li, A. Zhang, Q.L. Li, P.J.J. Alvarez, Polysulfone ultrafiltration membranes impregnated with silver nanoparticles show improved biofouling resistance and virus removal, Water Res. 43 (2009) 715–723.
[7] P.O. Rujitanaroj, N. Pimpha, P. Supaphol, Preparation, characterization, and antibacterial properties of electrospun polyacrylonitrile fibrous membranes containing silver nanoparticles, J. Appl. Polym. Sci. 116 (2010) 1967–1976.
[8] S. Liang, G. Qi, K. Xiao, J. Sun, E.P. Giannelis, X. Huang, M. Elimelech, Organic fouling behavior of superhydrophilic polyvinylidene fluoride (PVDF) ultrafiltration membranes functionalized with surface-tailored nanoparticles: implications for organic fouling in membrane bioreactors, J. Membr. Sci. 463 (2014) 94–101.
[9] A.L. Ahmad, A.A. Abdulkarim, B.S. Ooi, S. Ismail, Recent development in additives modifications of polyethersulfone membrane for flux enhancement, Chem. Eng. J. 223 (2013) 246–267.
[10] I. Voigt, J. Adler, M. Weyd, R. Kriegel, Ceramic filters and membranes, Ceramics Science and Technology, Wiley-VCH Verlag GmbH & Co. KGaA, 2013, pp. 117–167.
[11] S. Kroll, M. Oliveira, C. de Moura, F. Meder, G. Grathwohl, K. Rezwan, High virus retention mediated by zirconia microtubes with tailored porosity, J. Eur. Ceram. Soc. 32 (2012) 4111–4120.
[12] L. Treccani, M. Maiwald, V. Zollmer, M. Busse, G. Grathwohl, K. Rezwan, Antibacterial and abrasion-resistant alumina micropatterns, Adv. Eng. Mater. 11 (2009) B61–B66.
[13] C. Sengstock, M. Lopian, Y. Motemani, A. Borgmann, C. Khare, P.J.S. Buenconsejo, T.A. Schildhauer, A. Ludwig, M. Koller, Structure-related antibacterial activity of a titanium nanostructured surface fabricated by glancing angle sputter deposition, Nanotechnology 25 (2014).
[14] A. Ananth, G. Arthanareeswaran, A.F. Ismail, Y.S. Mok, T. Matsuura, Effect of biomediated route synthesized silver nanoparticles for modification of polyethersulfone membranes, Colloids Surf. A Physicochem. Eng. Asp. 451 (2014) 151–160.
[15] S. Chernousova, M. Epple, Silver as antibacterial agent: ion, nanoparticle, and metal, Angew. Chem. Int. Ed. 52 (2013) 1636–1653.
[16] J.R. Morones-Ramirez, J.A. Winkler, C.S. Spina, J.J. Collins, Silver enhances antibiotic activity against Gram-negative bacteria, Sci. Transl. Med. 5 (2013) 190ra181.
[17] S. Zhang, G. Qiu, Y.P. Ting, T.-S. Chung, Silver–PEGylated dendrimer nanocomposite coating for anti-fouling thin film composite membranes for water treatment, Colloids Surf. A Physicochem. Eng. Asp. 436 (2013) 207–214.
[18] C.N. Lok, C.M. Ho, R. Chen, Q.Y. He, W.Y. Yu, H.Z. Sun, P.K.H. Tam, J.F. Chiu, C.M. Che, Proteomic analysis of the mode of antibacterial action of silver nanoparticles, J. Proteome Res. 5 (2006) 916–924.
[19] A. Melaiye, W.J. Youngs, Silver and its application as an antimicrobial agent, Expert Opin. Ther. Pat. 15 (2005) 125–130.
[20] Y. Liu, E. Rosenfield, M. Hu, B. Mi, Direct observation of bacterial deposition on and detachment from nanocomposite membranes embedded with silver nanoparticles, Water Res. 47 (2013) 2949–2958.
[21] A. Nguyen, L. Zou, C. Priest, Evaluating the antifouling effects of silver nanoparticles regenerated by TiO_2 on forward osmosis membrane, J. Membr. Sci. 454 (2014) 264–271.
[22] S. Ghosh, R. Kaushik, K. Nagalakshmi, S.L. Hoti, G.A. Menezes, B.N. Harish, H.N. Vasan, Antimicrobial activity of highly stable silver nanoparticles embedded in agar–agar matrix as a thin film, Carbohydr. Res. 345 (2010) 2220–2227.
[23] C. Durucan, B. Akkopru, Effect of calcination on microstructure and antibacterial activity of silver-containing silica coatings, J. Biomed. Mater. Res. Part B 93B (2010) 448–458.
[24] D.Y. Koseoglu-Imer, B. Kose, M. Altinbas, I. Koyuncu, The production of polysulfone (PS) membrane with silver nanoparticles (AgNP): physical properties, filtration performances, and biofouling resistances of membranes, J. Membr. Sci. 428 (2013) 620–628.

[25] H. Basri, A.F. Ismail, M. Aziz, Polyethersulfone (PES)–silver composite UF membrane: effect of silver loading and PVP molecular weight on membrane morphology and antibacterial activity, Desalination 273 (2011) 72–80.
[26] J. Huang, G. Arthanareeswaran, K.S. Zhang, Effect of silver loaded sodium zirconium phosphate (nanoAgZ) nanoparticles incorporation on PES membrane performance, Desalination 285 (2012) 100–107.
[27] M. Sile-Yuksel, B. Tas, D.Y. Koseoglu-Imer, I. Koyuncu, Effect of silver nanoparticle (AgNP) location in nanocomposite membrane matrix fabricated with different polymer type on antibacterial mechanism, Desalination 347 (2014) 120–130.
[28] S. Silver, L.T. Phung, G. Silver, Silver as biocides in burn and wound dressings and bacterial resistance to silver compounds, J. Ind. Microbiol. Biotechnol. 33 (2006) 627–634.
[29] Y.H. Lv, H. Liu, Z. Wang, S.J. Liu, L.J. Hao, Y.H. Sang, D. Liu, J.Y. Wang, R.I. Boughton, Silver nanoparticle-decorated porous ceramic composite for water treatment, J. Membr. Sci. 331 (2009) 50–56.
[30] S. Kroll, L. Treccani, K. Rezwan, G. Grathwohl, Development and characterisation of functionalised ceramic microtubes for bacteria filtration, J. Membr. Sci. 365 (2010) 447–455.
[31] J.A. Creighton, C.G. Blatchford, M.G. Albrecht, Plasma resonance enhancement of Raman-scattering by pyridine adsorbed on silver or gold sol particles of size comparable to the excitation wavelength, J. Chem. Soc., Faraday Trans. 2 (75) (1979) 790–798.
[32] J.E. Doe, R.W. Lewis, P.A. Botham, Comments on A Scientific and Animal Welfare Assessment of the OECD Health Effects Test Guidelines for the Safety Testing of Chemicals under the European Union REACH System, ATLA, Altern. Lab. Anim. 34 (2006) 111–114.
[33] D.E. Reisner, Biotechnology II: Global Prospects, 2011.
[34] J. McFarland, The nephelometer: an instrument for estimating the numbers of bacteria in suspensions used for calculating the opsonic index and for vaccines, J. Am. Med. Assoc. 49 (1907).
[35] H.H. Lara, N.V. Ayala-Nunez, L.D.I. Turrent, C.R. Padilla, Bactericidal effect of silver nanoparticles against multidrug-resistant bacteria, World J. Microbiol. Biotechnol. 26 (2010) 615–621.
[36] V. Aruoja, H.-C. Dubourguier, K. Kasemets, A. Kahru, Toxicity of nanoparticles of CuO, ZnO and TiO_2 to microalgae *Pseudokirchneriella subcapitata*, Sci. Total Environ. 407 (2009) 1461–1468.
[37] U.S.E.P. Agency, Safe Drinking Water Act, http://water.epa.gov/lawsregs/rulesregs/sdwa/filterbackwash.cfm2013 (download 19/07/2013).
[38] J. Hasan, R.J. Crawford, E.P. Ivanova, Antibacterial surfaces: the quest for a new generation of biomaterials, Trends Biotechnol. 31 (2013) 295–304.
[39] D. Inbakandan, C. Kumar, L.S. Abraham, R. Kirubagaran, R. Venkatesan, S.A. Khan, Silver nanoparticles with anti microfouling effect: a study against marine biofilm forming bacteria, Colloids Surf. B: Biointerfaces 111 (2013) 636–643.
[40] H.C. Flemming, T.R. Neu, D.J. Wozniak, The EPS matrix: the "house of biofilm cells", J. Bacteriol. 189 (2007) 7945–7947.
[41] P. Paul, Development and testing of a fully adaptable membrane bioreactor fouling model for a sidestream configuration system, Membranes 3 (2013) 24–43.
[42] S. Asghari, S.A. Johari, J.H. Lee, Y.S. Kim, Y.B. Jeon, H.J. Choi, M.C. Moon, I.J. Yu, Toxicity of various silver nanoparticles compared to silver ions in *Daphnia magna*, J. Nanobiotechnol. 10 (2012).
[43] J. Kim, B. Van der Bruggen, The use of nanoparticles in polymeric and ceramic membrane structures: review of manufacturing procedures and performance improvement for water treatment, Environ. Pollut. 158 (2010) 2335–2349.
[44] W.H. Organization, Guideline for Drinking-water Quality — Silver in Drinking water, http://www.who.int/water_sanitation_health/dwq/chemicals/silver.pdf2003 (download 17/06/2013).
[45] W.L. Chou, D.G. Yu, M.C. Yang, The preparation and characterization of silver-loading cellulose acetate hollow fiber membrane for water treatment, Polym. Adv. Technol. 16 (2005) 600–607.